Biochimica et Biophysica Acta 1788 (2009) 1466–1473

Contents lists available at ScienceDirect

Biochimica et Biophysica Acta

journal homepage: www.elsevier.com/locate/bbamem

Role of acetylcholine receptor domains in ion selectivity

Chen Song, Ben Corry *

School of Biomedical, Biomolecular and Chemical Sciences, The University of Western Australia, Crawley WA 6009, Australia

ARTICLE INFO

Article history:
Received 23 January 2009
Received in revised form 9 April 2009
Accepted 21 April 2009
Available online 3 May 2009

Keywords:
Molecular dynamics
Brownian dynamics
nAChR
Ion channel
Membrane protein
Selectivity

ABSTRACT

The nicotinic acetylcholine receptor (nAChR) is a ligand gated ion channel protein, composed of three domains: a transmembrane domain (TM-domain), extracellular domain (EC-domain), and intracellular domain (IC-domain). Due to its biological importance, much experimental and theoretical research has been carried out to explore its mechanisms of gating and selectivity, but there are still many unresolved issues, especially on the ion selectivity. Moreover, most of the previous theoretical work has concentrated on the TM-domain or EC-domain of nAChR, which may be insufficient to understand the entire structure–function relation. In this work, we perform molecular dynamics, Brownian dynamics simulations and continuum electrostatic calculations to investigate the role of different nAChR domains in ion conduction and selectivity. The results show that although both the EC and IC domains contain strong negative charges that create large cation concentrations at either end of the pore, this alone is not sufficient to create the observed cation selectivity and may play a greater role in determining the channel conductance. The presence of cations in the wide regions of the pore can screen out the protein charge allowing anions to enter, meaning that local regions of the TM-domain are most likely responsible for discriminating between ions. These new results complement our understanding about the ion conduction and selectivity mechanism of nAChR.

1. Introduction

The nicotinic acetylcholine receptor (nAChR) belongs to the 'Cys-loop' family of ligand-gated ion channels which mediate synaptic neurotransmission [1]. The channel is found in high concentrations at the nerve–muscle synapse, where it mediates fast chemical transmission of electrical signals in response to acetylcholine (ACh) released from the nerve terminal into the synaptic cleft. Previous studies have shown that, like most of the other ion channels, nAChR is of crucial physiological importance and its malfunction is related to a number of known diseases including epilepsy, congenital myasthenia and muscle weakness [2]. Thus, understanding the conduction, selectivity and gating properties of the nAChR is highly desirable. However, although the genetics, kinetics, electrophysiology, and many topological aspects were well characterized for the nAChR [3,4], an atomic scale understanding of the protein has not been available until recent models have been developed based on 4 Å resolution maps obtained from cryoelectron microscopy (cryo-EM) [5,6]. The channel is made up from five homologous subunits packed around a central pore, forming a structure with fivefold pseudo-symmetry. Furthermore it is separated into three domains, namely, transmembrane domain (TM-domain), extracellular domain (EC-domain), and intracellular domain (IC-domain) as shown in Fig. 1a. TM-domain is the narrowest part of the pore which is embedded in the membrane, while EC-domain and IC-domain are much wider and form two large vestibules at both ends of the TM-domain. The radius of the pore is presented in Fig. 1b, with different domains marked.

Since the appearance of the experimentally determined structure of an ACh-binding protein and models of the *Torpedo* nAChR [5–7] much theoretical research has taken place to study the TM- and EC-domains as these are thought to play key roles in ligand binding, selectivity and gating. In particular these have investigated how the ACh binds to the EC-domain [8], how the EC-domain responds to the binding [9–11], how the conformation change of EC-domain is transferred to the TM-domain [12], and where and how the gating mechanism happens in the TM-domain [13–17]. Those theoretical works have provided many interesting findings in spite of the absence of the open state structure. While there has been some suggestion that the channel gate is located at the intracellular end of the TM-domain at the location of a number of charged or polar residues [18,19], a more common view is developing that the gate is midway across the membrane. Here there are a number of hydrophobic residues that may act to block ion permeation using a so called 'hydrophobic gating' mechanism by which a closed state pore is not necessarily physically blocked, and a small radius change can dramatically improve the water occupancy, which may lead to ion conduction [15,20–23].

However, in contrast to the numerous works on the gating mechanism of the EC-domain and TM-domain, few theoretical studies were carried out to explore the selectivity mechanism of the nAChR. The main reason is the absence of the detailed open-state structure. However, Ivanov et al's work showed us that, even by using the closed-state structure, we can obtain many useful clues which can give a reasonable explanation about the origins of ion selectivity [24].

* Corresponding author. Tel.: +61 8 6488 3166.
E-mail address: ben.corry@uwa.edu.au (B. Corry).

0005-2736/$ – see front matter © 2009 Elsevier B.V. All rights reserved.
doi:10.1016/j.bbamem.2009.04.015

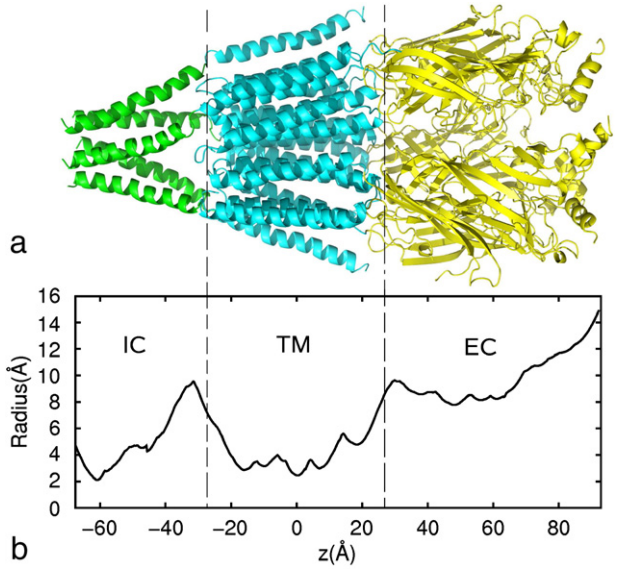

Fig. 1. (a) The refined cryo-electron microscopy structure of nAChR. The three domains are indicated with different colors, TM-domain in cyan, EC-domain in yellow, and IC-domain in green. (b) The radius of the channel, different domains are marked with dashed lines corresponding to (a).

Their conclusion that selectivity could be partially attributed to rings of charged residues at the extracellular and intracellular ends of the receptor pore and to the overall electrostatics of the TM-domain does sound reasonable, and it is consistent with many previous works which also highlight the effect of the charged residue rings on the ion conduction and selectivity [25–28]. However, the calculated electrostatic potential (ESP) of the TM-domain of the *Torpedo* nAChR cannot explain the cationic selectivity of this pore as shown below, indicating that other factors have to be taken into account. Additionally, Kienker et al. noted that the mutations on the charged extracellular and cytoplasmic rings of the TM-domain that influence conductance do not act by a simple electrostatic mechanism [29]. In addition mutations which can convert the ion selectivity of the channel from cationic to anionic [30,31] do not show distinct ESP changes, which implies that it is insufficient to understand the ion selectivity mechanism only from the ESP of TM-domain.

As a further complication, Unwin et al. already suspected that both extracellular and intracellular vestibules of the channel are strongly electronegative, providing a cation stabilizing environment at either entrance of the membrane pore [6]. The IC-domain may play an important role in selectivity by screening out ions of the wrong charge and size due to the narrow lateral windows. Indeed, some earlier experimental works have shown that not only the TM-domain [25,32], but also the IC-domain can determine the nAChR channel conductance [33]. However, the theoretical investigation of the IC-domain is totally absent so far. So it would be of great interest to study the possible selectivity property of the IC-domain as well. It is believed that we should not only consider the TM-domain when investigating the selectivity mechanism and conductance property of nAChR since the TM-domain is not isolated in the biological environment. Furthermore, there will be many ions residing inside this large protein that will influence the local ESP. Here we address the issue of whether the charged EC- and IC-domains play a role in ion selectivity, and if so how this can be reconciled with the fact that selectivity can be altered in this family of pores by a few mutations in the TM-domain. We find that the permeant ions play a large role in determining the field in this pore, and electrostatic profiles for either the TM-domain in isolation or the entire nAChR calculated in their absence do not provide useful information about ion selectivity. It will be shown that although the EC and IC-domains create a region of high cation concentration this is not sufficient to explain the observed degree of selectivity.

In this work, we perform extensive theoretical studies to investigate what role each domain of the *Torpedo* nAChR plays in ion selectivity and conductance. Specifically, continuum electrostatic calculations are carried out to examine if the ESP resulting from TM-domain can explain the experimentally observed ion selectivity. We study the water occupancy and *I–V* curve of EC-domain to evaluate its likely ion conductance and selectivity property. We perform potential of mean force (PMF) calculations on the IC-domain to give a quantitative description of its 'screening' function. Finally, we give an overall description of the role of acetylcholine receptor domains in ion conduction and selectivity. Using a 'segmented' approach in which each domain is studied individually allows for much longer simulations to be conducted, which is particularly necessary for doing the PMF calculations. It is also useful to evaluate the ion conductance of the 'isolated' EC-domain. But our study also shows that, the 'segmented' approach should be carefully used since sometimes important information may be lost, as seen in the electrostatic calculations of TM-domain.

2. Methods

2.1. MD simulations

MD simulations were performed starting with the refined structure of the nAChR (Protein Data Bank entry 2BG9) [6]. We separated the protein into three domains and performed MD simulations on each of them respectively. We also performed MD simulations on the entire nAChR embedded in a fully hydrated POPC bilayer. The protein was separated into three domains for simulation by selecting residues from the α-subunit along with residues with a corresponding range of *z* coordinates from the other subunits. For the TM-domain, residues P211-H306 and K400-G437 of the α-subunit were selected while for the EC-domain we used residues S1-I210. For the IC-domain, we included the intracellular exit of the TM channel along with the IC-domain. Thus, residues V230-S248, V294-H306 and S374-M415 were chosen.

Before performing MD simulations on the TM-domain, we placed it within a POPC lipid membrane and solvated the system with the TIP3 water molecules, to which we added 26 Cl^- and 25 Na^+ ions to get a neutral system, resulting in a $117\times117\times83$ $Å^3$ water box with about 0.15 M ion concentration (105,720 atoms altogether). Water was initially placed within the pore. The lipid and water was initially energy minimized for 50,000 steps and equilibrated for 20 ps with the protein held fixed. Then harmonic constraints were applied to the α-carbon atoms of the protein, and a further 5000 steps of energy minimization and 20 ps of equilibration were performed. Finally all constraints were released and the system was energy minimized for 5000 steps and 60 ps of simulation was conducted before data collection of the 5-ns production run.

For the MD simulations of EC- and IC-domains, the protocols were relatively simple. First, the molecule was solvated in a TIP3 water box, which was then neutralized with Na^+ and Cl^- ions to get the ion concentration to 0.15 M. Then the systems were relaxed with gradually decreasing harmonic constraints on the protein. Finally the water box containing the EC-domain was simulated with a production run of 5 ns, without any restraints. For the production run of IC-domain, the end residues which would be connecting to the TM-domain were all fixed.

Since the wide radius of EC pore allowed water occupation to be well sampled in this region, the PMF for water molecules in the pore of EC-domain was calculated directly from the water oxygen probability distribution obtained from equilibrium simulations using the fact that $P(z)\propto\frac{e^{-G(z)}}{kT}$ [34,35]. Here $P(z)$ was taken as the total number of water

molecules located within 20 Å of the axis of the EC vestibule. Calculations were made using the implementation of Grossfield [36].

PMF calculations for the ions (Na^+/Cl^-) going through a lateral window of the IC-domain were performed by using umbrella sampling [37], in which a harmonic biasing potential was applied to the test ion. The target position was moved along a reaction coordinate ξ passing through one of the lateral entrances from ξ = −15 to ξ = 10 Å (the backbones locate at the position of ξ = −5 to −3 Å) using force constants $k_\xi = 2.0$ and $k_c = 0.5$ kcal mol$^{-1}\cdot$Å^{-2} (k_c means a cylindrical confining potential was applied in order to prevent the ion from drifting too far from the path we are interested in). The reaction coordinate ξ was selected to pass through the center of the lateral window, and be perpendicular to the surface of the lateral window. The width of sampling windows was chosen to be 1 Å, and 500 ps simulation was performed for each window. Collective analysis of the data was made using the weighted histogram analysis method [34,35], using the implementation of Grossfield [36]. Weak restraints were applied to all the α-carbon atoms of the IC-domain residues.

Finally, we performed MD simulations on the entire nAChR, which was embedded in POPC lipid membrane and solvated in a solution with 0.15 M ion concentration (233,175 atoms altogether). Similar protocols to that of TM-domain was adopted, and the production run was performed for 5 ns. A comparison 5-ns MD simulation was performed for one mutated nAChR (according to the selectivity conversion mutations, see below).

All the MD simulations were performed using periodic boundary conditions with the NAMD2 program [38] using the CHARMM27 force field [39]. A short-range cutoff of 12 Å was used for nonbonded interactions, and the long-range electrostatic interactions were calculated with particle mesh Ewald method [40,41]. Langevin dynamics and a Langevin piston algorithm were used to maintain the temperature at 310 K and a pressure of 1 atm. The time step was set to 1 fs.

It should be noted that in this study we assume the heterogeneity of the lipid has little effect on the simulation results in term of the purpose of the study, because the nAChR channel has reasonably thick walls and the electrostatic potential inside the pore is not likely to be influenced by the exact structure of the lipid. Unresolved residues in the IC-domain of the cryo-EM model were not included in any simulations.

2.2. BD simulations

The conductance of the EC-domain as well as the ion distribution of the whole system were calculated explicitly using BD simulations, which has been successfully applied to the nAChR and other channels [15,42]. The motion of individual ions is traced explicitly, but the water and protein atoms are treated as continuous dielectric media [43,44]. The channel is taken to be a rigid structure during the simulation, and partial charges are assigned to the protein using the CHARMM all atom parameter set. The pore is centred on the *z*-axis and a smooth water–protein boundary of the channel is defined by rolling a 1.4 Å sphere representing the water molecule along the surface. The boundary is symmetrised by taking only the minimum radius at each *z*-coordinate, and then the curve is rotated by 360° to obtain a three-dimensional channel structure with radial symmetry. A number of Na^+ and Cl^- ions are placed in cylindrical reservoirs of radius 30 Å at each end of the channel that mimic the intra- and extra-cellular solution, and the height of the cylinder is adjusted to bring the solution to the desired concentration. The motion of these ions under the influence of electric and random forces is then traced using the Langevin equation. The total force acting on each and every ion in the assembly is calculated and then new positions are determined for the ions a short time later. Electrostatic forces are calculated by assigning dielectric constants of 2 to the protein and 60 to the water in the channel and solving Poisson's equation using an iterative method [45]. It should be noted that while the dielectric constant of bulk water is close to 80, this is likely to be reduced in the confined space inside the pore. Unfortunately, it is difficult to establish the appropriate value of the dielectric constant *a priori*. The values of the dielectric constants chosen in this study have been established to give the best agreement with experimental currents in a range of situations [46–49]. To examine the influence of the choice of dielectric constant on our results we have also performed BD simulations with a dielectric constant of water set to 80. Under these conditions the resulting difference in the ion conductance through the EC-domain was less than 1% as was the difference in ion concentrations seen in the simulations of the entire nAChR. The current is determined directly from the number of ions passing through the channel. The membrane potential is achieved by applying a uniform filed to the system and is incorporated into the solution of Poisson's equation. More details about the BD simulation can be found in previous studies [15,43,44].

BD simulations were performed for EC-domain and the whole nAChR system respectively. When performing BD simulations for the EC-domain, we adopted a series of electric field values to obtain the *I–V* curves. We performed grand canonical Monte Carlo BD simulations for the entire nAChR with no applied electric field to determine the equilibrium ion distribution. In this, the grand canonical Monte Carlo scheme was used to maintain the desired ion concentrations in the reservoirs by creating or destroying ions near the edge of the reservoirs in a random manner dependent on the local electrochemical potential [50]. As the BD method is currently designed for systems with axial symmetry we could not simulate the IC-domain that has lateral windows. In order to simulate the entire protein the very internal end of the IC-domain was truncated to open an axial entrance to the pore. Please note that the truncation results in an incomplete structure with large opening of IC-domain to the intracellular solvent, which is likely to lead to a higher permeability through this region.

2.3. Others

Electrostatic potential calculations were carried out using the APBS (Adaptive Poisson–Boltzmann Solver) package [51] using charges from the CHARMM27 force field, where saline and lipid environments were not considered, and the aspartic acid, glutamic acid, and histidine are all set to be deprotonated in line with the MD simulations. The detailed set of calculation parameters included: protein dielectric of 2.0, solvent dielectric of 78.54, solvent radius 1.4 Å, temperature of 298.15 K, ion concentration of 0.0 M, grid dimensions of 193 × 193 × 353, and grid spacing ~0.5 Å.

Mutations to the protein were constructed using the program 'nest' [52], following the three site-mutations that have been shown to convert neuronal nAChR's selectivity from cationic to anionic [30] as shown in Fig. 2. The pore radii were calculated using the program 'HOLE' [53], and the program VMD [54] and PyMOL [55] were used in the visualization and analysis of the results.

3. Results and discussions

3.1. Study of the TM-domain

First, we performed MD simulation for the TM-domain according to the method described above. The evolution of the root mean

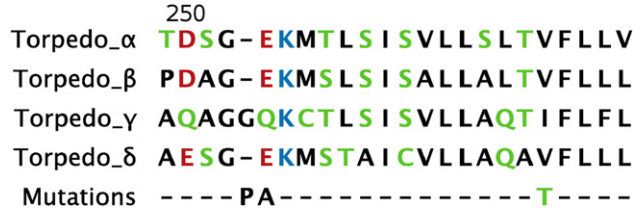

Fig. 2. Three site mutations applied to the *Torpedo* nAChR model.

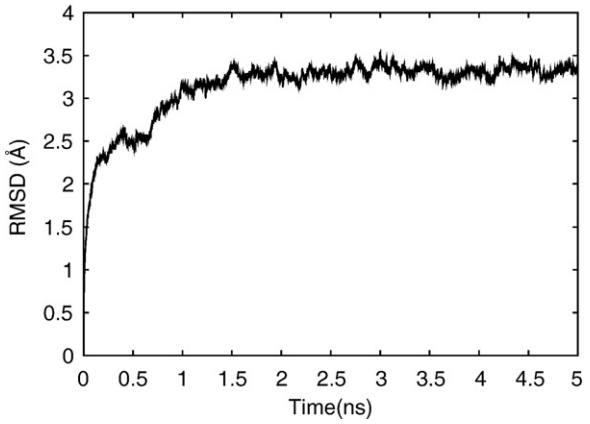

Fig. 3. Evolution of the RMSD value from the starting structure for MD simulation of the TM-domain.

squared deviation (RMSD) of the protein (calculated only for nonhydrogen atoms) is shown in Fig. 3. As can be seen, the simulation reaches a stable stage after 2-ns (out of a total 5 ns) of simulation, with an average RMSD value about 3.25 Å, showing that the experimental structure is relatively stable under our simulation protocol. Previous studies have shown that there is a hydrophobic girdle in the TM-domain, which is believed to be responsible for the 'hydrophobic' gating mechanism [15,22]. In our simulations, we also find that this hydrophobic region, which extends from L251 to V259 of the α subunit, restricts water occupancy in the pore, and is therefore likely to prevent the passage of ions. The water density in this region is much lower than in bulk and is often evacuated despite starting with water throughout the pore. We do not want to go further to study the gating mechanism of the channel, which has been done by many other works.

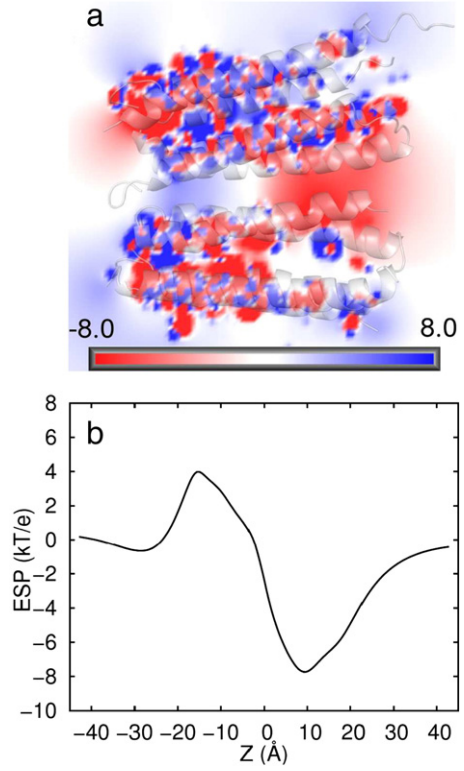

Fig. 4. The electrostatic potential of the TM-domain (in kT/e), (a) the slice crossing the channel axis. The extracellular entrance is to the right hand. (b) the profile along the channel axis. The positive direction of z axis points to the extracellular entrance.

According to Ivanov et al.'s study, the electrostatics and the presence of rings of charged residues at the entrance and exit of the TM-domain may play an important role in ion selectivity of the neuronal α7 receptor [24]. Here we also performed ESP calculations on our model of the *Torpedo* protein trying to explore the selectivity mechanism of the TM-domain, but the results showed an unexpected character. As can be seen in Fig. 4, the extracellular entrance of the TM-domain has a negative potential, where it is attractive for Na^+ ions; but the intracellular entrance of the TM-domain has a positive potential, which will repel Na^+. This is different to Ivanov et al's results for the α7 receptor where both entrances have negative potential. Considering the fact that the sequences are different, it is easy to understand since there are more lysines than glutamic acids at the IC-entrance of the *Torpedo* structure resulting in a slight positive potential in our case. But this cannot explain the ion selectivity mechanism from the electrostatic potential viewpoint. It may be necessary to consider not only the electrostatic effect of the TM-domain, but also the remainder of the protein and even the environment to gain the complete picture. Alternatively, the ESP calculated in this way may not provide useful information regarding ion selectivity. We will discuss this in more detail in the following sections.

3.2. Study of the EC-domain

After performing a 5-ns MD simulation, the isolated EC-domain maintained its regular cylindrical structure, but the pore shrank slightly with the average radius changing from 9.1 Å to 7.6 Å. The average structure of the last nanosecond simulation, colored with the RMSD of each residue is shown in Fig. 5 (red refers to more mobile residues and blue less mobile ones). Both the side view and top view show that the α-helix regions are more flexible than the β-sheet region. The pore radius of the EC-domain is much wider than that of TM-domain, with the minimum radius more than 5 Å near the entrance to the TM-domain as shown in Fig. 6a. Due to the wide radius of the extracellular-domain, water molecules and ions are found to be able to occupy the interior of the pore easily in MD simulations, and the potential of mean force they encounter can be calculated from equilibrium simulations.

Not surprisingly, the PMF calculation of water in the EC-domain pore shows only small barrier, about 0.6 kcal/mol, located roughly where the pore is narrowest, as shown in Fig. 6b. The PMF values in the pore fluctuate from 0.3 to 0.6 kcal/mol depending on the radius of the pore, consistent with that for the simple non-polar carbon nanotube model pore with similar dimensions [56]. But due to the high polarity of the surrounding residues, we expect a higher conductance than that of the hydrophobic nanotube.

Correspondingly, the BD results also show that it is easy for Na^+ and Cl^- ions to pass through the EC-channel. We counted the ions passing through the EC-domain under different voltages, and

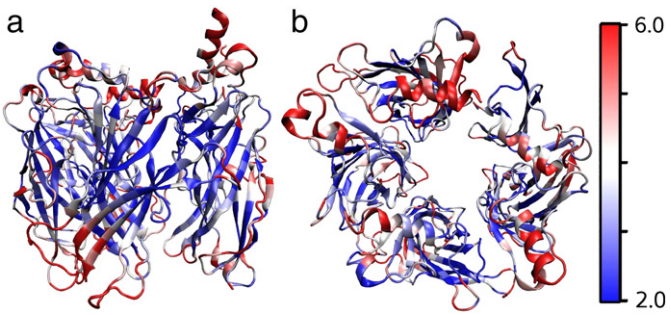

Fig. 5. The side view (a) and top view (b) of the EC-domain, colored according to the RMSD of each residue, as shown by the scale bar.

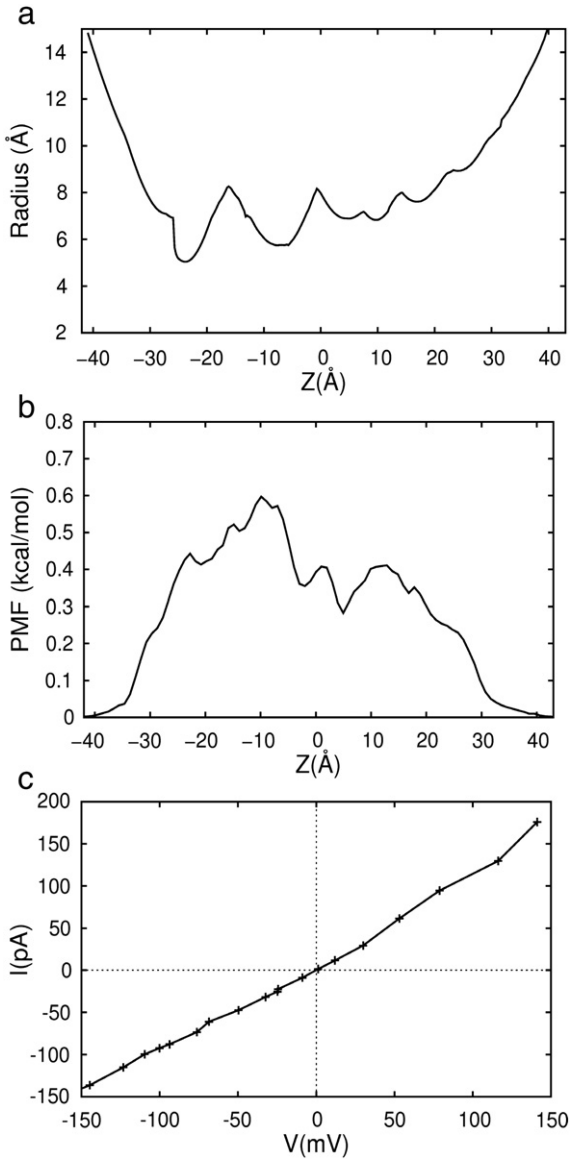

Fig. 6. Simulations of the EC-domain. (a) The pore radius of EC-domain, (b) the PMF of water in EC-domain calculated from MD simulations, the origin of (a) and (b) represents the center of the EC-domain along *Z* axis, and (c) the *I–V* curves of EC-domain calculated from BD simulations.

calculated the *I–V* curve of the EC-domain, which is shown in Fig. 6c. We can see the EC-domain has a very high conductance of about 1.25 nS. Notably, it is much higher than the experimental values for the entire nAChR [57], indicating that the rate limiting step to ion permeation must occur elsewhere [25,32]. Thus the EC-domain, even in the nAChR closed state, is a high-conductance channel, and does not act to directly gate the passage of ions.

A notable feature of the EC-domain is that it is highly negatively charged. According to the previous studies, a negatively charged channel would be expected to be cation selective [4]. In our BD simulations, both Na^+ and Cl^- ions can pass through the EC-channel, but Na^+ does so at a higher rate than Cl^-, which depends on the external field. Furthermore, the Na^+ concentration in the EC-domain is much higher than Cl^- concentration, resulting in a high Na^+ concentration at the entrance of the TM-domain (see below).

These results highlight the fact that a highly negatively charged pore may create larger concentrations of cations than anions, but need not prevent anion conductance altogether in such a wide pore. As the EC-domain fills with Na^+, the ESP will be equalized to allow entry of the anions. This is in rough agreement with Meltzer et al.'s study, in which negative charges are also found in the EC vestibule [58]. While the EC-domain is unlikely to determine the hundred fold selectivity of the pore, it may dictate the rate of cation conductance through the adjacent TM-domain as well as containing the ligand binding site. It is interesting to see Hansen et al's recent experimental study, which also indicates that the EC-domain plays a function role in stabilizing the permeant ions within the extracellular vestibule of nAChR, which is a major determinant of ion conductance [59]. This is consistent with our theoretical results.

3.3. Study of the IC-domain

During the MD simulation of the IC-domain, we found that a number of Na^+ ions accumulated in the IC-domain vestibule. In contrast, all Cl^- ions remained outside. This reminds us of Unwin et al.'s hypothesis that IC-domain may act as an electrostatic filter [6], so we calculated the ESP of the IC-domain and plotted this on the solvent accessible surface as shown in Fig. 7a. The red color refers to negative potential, while the blue color means a positive potential. It is very obvious that the whole entrance/exit of the IC-domain is negatively charged due to the existence of glutamic acids. No doubt this assists the passage of Na^+ into the intracellular vestibule.

To give a rough quantitative description of the IC-domains function as an electrostatic filter, we performed PMF calculations for translocation of Na^+ and Cl^- ions into the vestibule as shown in Fig. 7b. In this, ions are moved through one of lateral windows along the direction of the arrow indicated in the Fig. 7a, with the ion position

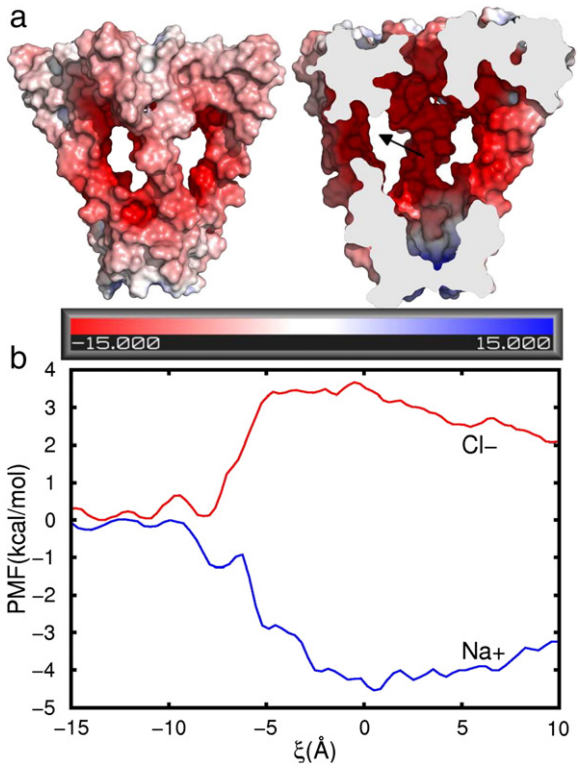

Fig. 7. Simulations of the IC-domain. (a) Cross sections showing the outer and inner solvent accessible surfaces of intracellular vestibule colored according to the electrostatic potential on the surface (positive potential is blue and negative is red, in kT/e). The arrow shows the reaction coordinates along which the PMF was calculated. (b) The potential of mean force for Na^+ and Cl^- ions entering the intracellular vestibule through one of the lateral windows (ξ-axis corresponds to the reaction coordinate, negative coordinate is outside of the vestibule, and the positive end is the center of the vestibule).

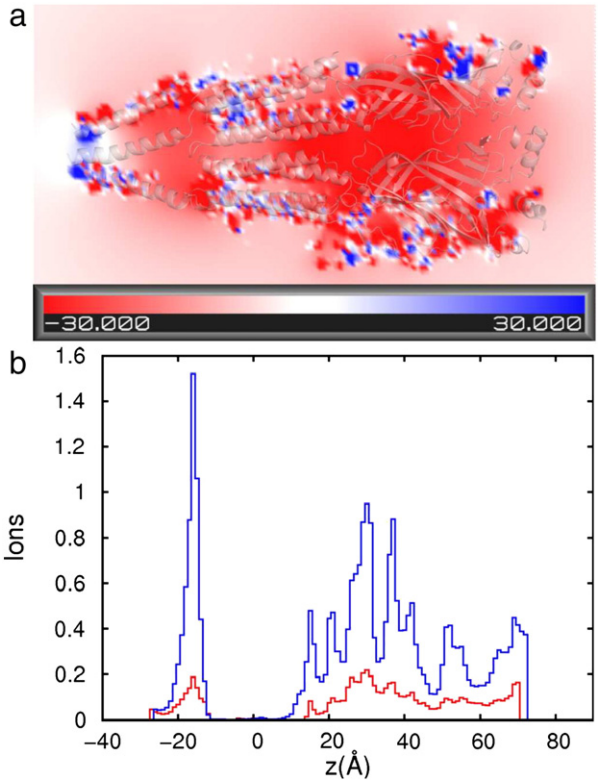

Fig. 8. Simulations of the entire nAChR. (a) A slice, which crosses the pore axis, showing the electrostatic potential (in kT/e). (b) the average ion distribution in the nAChR from BD simulations, Na^+ in blue and Cl^- in red.

noted by the reaction coordinate ξ. The negative direction of the ξ-axis corresponds to the outside of the IC-domain, while the positive direction means the inside of the IC-domain. The α helix backbones (i.e. the center of the window) are located between $\xi = -5$ and -3 Å in this plot. It is very distinct that for the Na^+ ions, it is energetically favorable to stay inside of the vestibule, and the most steady positions for Na^+ ions are the locations about 3– 5 Å from the backbones inside the vestibule. While for the Cl^- ions, it is more energetically favorable for them to stay outside of the vestibule. The potential well for Na^+ is about 5.3 kcal/mol deep, and the potential barrier for Cl^- is about 3.6 kcal/mol high. These results clearly indicate that the IC-domain actually has 'filter' function. It will try to keep Cl^- ions outside of the vestibule and keep the Na^+ ion concentration at a higher level in the vestibule.

Our results suggest that the IC-domain does act as an electrostatic filter. Like with the EC-domain, this may contribute to determining the conductance of nAChR since it can determine the ion concentration at the IC-entrance to the TM-domain. In addition it would make a barrier for Na^+ ions to come out of the vestibule, which is the last step of inward ion transport. Indeed, previous experimental work on another channel of 'Cys-loop' family, 5-Hydroxytryptamine type 3 ($5\text{-}HT_3$), showed that mutations on a cytoplasmic region can increase single-channel conductance 28-fold by changing positively charged residues to neutral or negatively charged residues [33]. We expect that a similar situation can occur in nAChR, i.e., mutations on the glutamic acids of IC-domain to neutral or positively charged residues may alter the single-channel conductance of nAChR and its rectification properties.

It should be kept in mind that the IC-domain structure in the cryo-EM model is not complete with a number of residues unresolved, which were therefore not included in our simulations and may influence the calculated PMF. But, the current study does provide interesting information on the filtering role of this domain consistent with previous experimental results. To the best of our knowledge, this is the first time that MD simulations are carried out to evaluate the function of this IC-domain. A high resolution structure of the complete IC-domain is needed to yield more complete quantitative results.

3.4. Study of the entire nAChR

So far we have described studies on the separate domains of nAChR. Finally, we will combine them together and give an overall consideration of the protein. We performed 5-ns MD simulation for the entire nAChR, and found that only Na^+ ions are seen to accumulate in the EC-domain channel and IC-domain vestibule, around the entrances to the TM-domain. Combined with the above results, this may suggest that not only the TM-domain, but also the EC- and IC-domains are responsible for determining the conductance of the channel. But, as the BD simulations on the EC-domain demonstrate, the large charge on these domains may not prevent anion conductance entirely as described below.

We calculated the ESP of the entire structure, as shown in Fig. 8a. The results show that the potential is negative throughout the EC-channel to the IC-vestibule. This contrasts with results we have shown in the previous section that the ESP at the IC-entrance is positive, which emphasizes the role that the additional domains can play in determining the ESP (in the absence of permeating ions). Considering the experimental observation that only three residue mutations are required to convert the ion selectivity of the channel [30,31], we wanted to explore the effect of the mutations on the ESP of the entire nAChR and performed ESP calculations on the mutated nAChR. We do find some changes in the ESP after mutations as shown in Fig. 9. The most obvious change is around the mutation sites ($-20<z<-10$), where the ESP increased about 10 kT/e after mutations. However, the ESP value at the intracellular entrance region of TM-domain is still negative even after mutations. The selectivity of the channel cannot therefore be entirely dictated by the ESP of protein itself. This leads to two possible solutions for understanding how three mutations can so drastically alter the selectivity of an nAChR. One explanation is that conformational changes after mutations play the key role in selectivity. We performed MD simulations on the mutated nAChR, but there are no obvious changes found in the short simulations we could undertake on the closed state model. However, it is still possible that the mutations can have an effect in the open state of the channel.

Another possibility is to realize that a wide highly charged region of the pore (such as the EC-domain) can still allow both ion types to pass, as witnessed in BD simulations of the EC-domain alone. This means that the ESP of a localised region (such as inside the TM-domain) could then dictate selectivity rather than the overall ESP, as suggested by Meltzer et al. [58,60]. We also performed grand canonical Monte Carlo BD simulations [50] for the entire nAChR

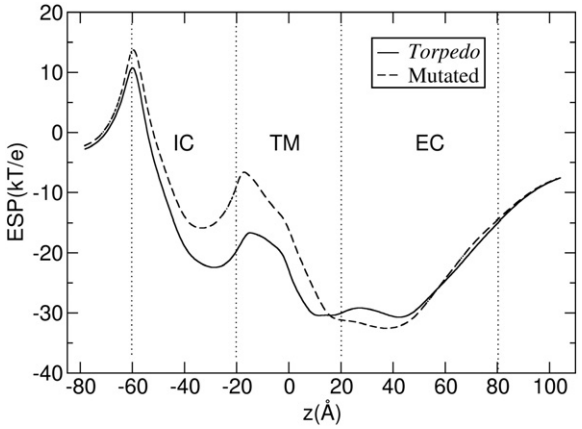

Fig. 9. The electrostatic potential profiles along the channel axis through the wild type *Torpedo* and the mutated structure. The three domains are marked with dot lines.

without any external electric field and calculated the average distribution of ions in the pore after Na^+ and Cl^- reached equilibrium densities in the simulations. The result is shown in Fig. 8b, where we can see many Na^+ ions accumulating in the EC-domain and IC-domain, around the entrance to the TM-domain. However, there are still some Cl^- ions seen in both domains, although much less than Na^+ ions. In the IC-domain we find about 6 Na^+ and 2 Cl^-, while there are about 20 Na^+ and 5 Cl^- in the EC domain. We analyzed the simulation trajectory, and found that at the first stage of the simulation, only Na^+ ions can access the EC-channel and IC-vestibule, but as time goes on, when more Na^+ ions accumulate in the channel, Cl^- ions also gradually go into the channel due to the gradually evened ESP (not seen in the MD simulation due to the time scale limit). Thus, both EC- and IC-domain have the ability to maintain high Na^+ ion concentration, which will help to determine the conductance of the nAChR. This is consistent to Unwin's suspicion that both vestibules of the channel are strongly electronegative, providing a cation stabilizing environment at either entrance of the membrane pore. However, if the TM-domain had no role in selectivity, then these concentrations in the EC and IC domains could be expected to yield a permeability ratio of Na^+:Cl^- of only 3– 4, well below the experimentally measured value. The presence of Cl^- in the EC-domain allows for the possibility that small local changes in the ESP or conformation in the TM-domain, such as induced by just three mutations, could be enough to enable the passage of Cl^- and/or block Na^+. It would be ideal to calculate the channel current in the presence and absence of the EC-domain to determine the likely selectivity in each case. Unfortunately, this is not possible currently as we only have a closed state experimental TM-domain structure that will not conduct ions in either case, even if huge external voltage was applied in BD simulations. However, we believe the fact that anions can permeate through the EC-domain alone, and that they occupy the EC-domain when we simulate the entire channel clearly shows that the EC-domain does not exclude anions.

It is very obvious that only considering part of the system in electrostatic calculation is not enough to give a reasonable explanation about selectivity as our electrostatic results for TM-domain and for the whole structure are very different. Furthermore the counter ions must also be taken into account to explore the origin of the ion selectivity. The use of explicit ion models such as in BD is particularly important for gaining reliable electrostatic profiles. Poisson's equation does not account for counter-ions and continuum electrolyte descriptions such as the Poisson–Boltzmann equation have previously been shown to be faulty in narrow pores [61]. Examining the ESP of the protein in the absence of the permeant ions does not give a clear indication of the origins of ion selectivity.

It should be noted that in our MD simulations and ESP calculations we did not consider any pK_a shifts which might also affect the ESP results. We also note Brannigan et al.'s recent work, in which they show that the nAChR contains internal sites capable of containing cholesterol, whose occupation may stabilize the protein structure [62]. Indeed, we also found shrinkage of the TM-domain when performing MD simulations on the entire system without cholesterol, which is consistent with their observation. However, like most of the other MD works on nAChR, we did not take this into account since it is not likely to influence the basic conclusion regarding ion occupancy and selectivity of different domains.

4. Summary

In this study, we performed electrostatic calculations, MD and BD simulations on the three domains of nAChR in isolation, as well as the entire nAChR structure, to explore the role each of the domains has in ion conduction and selectivity. Our results suggest that although the EC-domain and IC-domain are negatively charged and create a fourfold excess of cations over anions, this is not sufficient to explain the selectivity of the pore considering that it is effectively impermeable to anions [63]. The fact that counter ions can enter the vestibules helps to understand the finding that just a few mutations in the TM-domain can change the channel selectivity from cationic to anionic. The EC-domain in particular is very wide and counter ions can screen the charge on the protein allowing both cation and anions to enter. It is therefore misleading to use the ESP in the channel determined in the absence of permeating ions to make inferences about ion selectivity. The charged EC- and IC-domains do, however, create large cation concentrations at either end of the TM domain of the pore that will increase their conductance.

Once anions are inside the EC-domain, their conductance through the pore can be dictated by properties of the TM-domain. Therefore the TM-domain seems most likely to be responsible for the majority of cation selectivity, consistent with mutation experiments. However, one can not give a clear picture about selectivity only by studying the TM-domain, or even the whole structure without considering the environment and flexibility of the pore. In this work we conduct extensive theoretical simulations to help justify a possible mechanism of ion selectivity that can account for the fact that mutations in the TM region can reverse cation/anion discrimination despite the fact that the EC- and IC-domains remain negatively charged. Future work utilizing an open state structure of a nicotinic acetylcholine receptor including all residues in the IC domain will be required to give a more definite explanation of ion selectivity.

The atomic resolution X-ray structures of prokaryotic pentameric ligand gated ion channels have recently been published, in which no IC-domain is seen and the channel appears to be physically occluded in the closed state [64]. These characteristics are very different from the *Torpedo* nAChR and human α7 receptor models based on the cryo EM data and raise interesting questions about whether the differences are due to the underlying sequence differences or reside in the measurement conditions and models. The availability of such atomic resolution data, especially those for the apparently open conformation channel [65,66], are likely to promote a new impetus into the structural studies of this family of proteins.

Acknowledgements

This work is supported by funding from the National Health and Medical Research Council of Australia, an award under the merit allocation scheme on the APAC National Facility at the ANU and additional computer time from iVEC.

References

[1] S.M. Sine, A.G. Engel, Recent advances in Cys-loop receptor structure and function, Nature 440 (2006) 448–455.
[2] F.M. Ashcroft, From molecule to malady, Nature 440 (2006) 440–447.
[3] P.C. Jordan, Fifty years of progress in ion channel research, IEEE T, NanoBiosci. 4 (1) (2005) 3–9.
[4] P.H. Barry, J.W. Lynch, Ligand-gated channels, IEEE T. NanoBiosci. 4 (1) (2005) 70–80.
[5] A. Miyazawa, Y. Fujiyoshi, N. Unwin, Structure and gating mechanism of the acetylcholine receptor pore, Nature 423 (2003) 949–955.
[6] N. Unwin, Refined structure of the nicotinic acetylcholine receptor at 4 Å resolution, J. Mol. Biol. 346 (2005) 967–989.
[7] K. Brejc, W.J. van Dijk, R.V. Klaassen, M. Schuurmans, J. van der Oost, A.B. Smit, T.K. Sixma, Crystal structure of an ach-binding protein reveals the ligand binding domain of nicotinic receptors, Nature 411 (2001) 269–276.
[8] D. Zhang, J. Gullingsrud, J.A. McCammon, Potentials of mean force for acetylcholine unbinding from the alpha7 nicotinic acetylcholine receptor ligand-binding domain, J. Am. Chem. Soc. 128 (2006) 3019–3026.
[9] R.H. Henchman, H.-L. Wang, S.M. Sine, P. Taylor, J.A. McCammon, Asymmetric structural motions of the homomeric α7 nicotinic receptor ligand binding domain revealed by molecular dynamics simulation, Biophys. J. 85 (2003) 3007–3018.
[10] R.H. Henchman, H.-L. Wang, S.M. Sine, P. Taylor, J.A. McCammon, Ligand-induced conformational change in the α7 nicotinic receptor ligand binding domain, Biophys. J. 88 (2005) 2564–2576.
[11] F. Gao, N. Bren, T.P. Burghardt, S. Hansen, R.H. Henchman, P. Taylor, J.A. McCammon, S.M. Sine, Agonist-mediated conformational changes in acetylcholine-binding protein revealed by simulation and intrinsic tryptophan fluorescence, J. Biol. Chem. 280 (2005) 8443–8451.

[12] X. Cheng, H. Wang, B. Grant, S.M. Sine, J.A. McCammon, Targeted molecular dynamics study of C-loop closure and channel gating in nicotinic receptors, PLOS Comput. Biol. 2 (9) (2006) 1173–1184.
[13] B. Corry, Theoretical conformation of the closed and open states of the acetylcholine receptor channel, Biochim. Biophys. Acta 1663 (2004) 2–5.
[14] R.J. Law, R.H. Henchman, J.A. McCammon, A gating mechanism proposed from a simulation of a human α7 nicotinic acetylcholine receptor, Proc. Natl. Acad. Sci. U. S. A. 102 (19) (2005) 6813–6818.
[15] B. Corry, An energy-efficient gating mechanism in the acetylcholine receptor channel suggested by molecular and Brownian dynamics, Biophys. J. 90 (2006) 799–810.
[16] X. Cheng, B. Lu, B. Grant, R.J. Law, J.A. McCammon, Channel opening motion of α7 nicotinic acetylcholine receptor as suggested by normal mode analysis, J. Mol. Biol. 355 (2006) 310–324.
[17] A. Taly, M. Delarue, T. Grutter, M. Nilges, N.L. Novère, P.-J. Corringer, J.-P. Changeux, Normal mode analysis suggests a quaternary twist model for the nicotinic receptor gating mechanism, Biophys. J. 88 (2005) 3954–3965.
[18] G.G. Wilson, A. Karlin, The location of the gate in the acetylcholine receptor channel, Neuron 20 (1998) 1269–1281.
[19] J. Pascual, A. Karlin, State-dependent accessibility and electrostatic potential in the channel of the acetylcholine receptor: inferences from rates of reaction of thiosulfonates with substituted cysteines in the M2 segment of the alpha subunit, J. Gen. Physiol. 111 (1998) 717–739.
[20] O. Beckstein, P. Biggin, M. Sansom, A hydrophobic gating mechanism for nanopores, J. Phys. Chem. B 105 (2001) 12902–12905.
[21] O. Beckstein, P.C. Biggin, P. Bond, J.N. Bright, C. Domene, A. Grottesi, J. Holyoake, M. S. Sansom, Ion channel gating: insights via molecular simulations, FEBS Lett. 555 (2003) 85–90.
[22] O. Beckstein, M.S.P. Sansom, A hydrophobic gate in an ion channel: the closed state of the nicotinic acetylcholine receptor, Phys. Biol. 3 (2006) 147–159.
[23] G.D. Cymes, C. Grosman, Pore-opening mechanism of the nicotinic acetylcholine receptor evinced by proton transfer, Nat. Struct. Mol. Biol. 15 (2008) 389–396.
[24] I. Ivanov, X. Cheng, S.M. Sine, J.A. McCammon, Barriers to ion translocation in cationic and anionic receptors from Cys-loop family, J. Am. Chem. Soc. 129 (2007) 8217–8224.
[25] K. Imoto, C. Busch, B. Sakmann, M. Mishina, T. Konno, J. Nakai, H. Bujo, Y. Mori, K. Fukuda, S. Numa, Rings of negatively charged amino acids determine the acetylcholine receptor channel conductance, Nature 335 (1988) 645–648.
[26] T. Konno, C. Busch, E. Vonkitzing, K. Imoto, F. Wang, J. Nakai, M. Mishina, S. Numa, B. Sakmann, Rings of anionic amino-acids as structural determinants of ion selectivity in the acetylcholine-receptor channel, P. Roy. Soc. B—Biol. Sci. 244 (1991) 69–79.
[27] J.D. Lear, J.P. Schneider, P.K. Kienker, W.F. DeGrado, Electrostatic effects on ion selectivity and rectification in designed ion channel peptides, J. Am. Chem. Soc. 119 (1997) 3212–3217.
[28] B. Corry, S. Chung, Mechanisms of valence selectivity in biological ion channels, Cell. Mol. Life Sci. 63 (2006) 301–315.
[29] P. Kienker, G. Tomaselli, M. Jurman, G. Yellen, Conductance mutations of the nicotinic acetylcholine receptor do not act by a simple electrostatic mechanism, Biophys. J. 66 (1994) 325–334.
[30] J.-L. Galzi, A. Devillers-Thiéry, N. Hussy, S. Bertrand, J.-P. Changeux, D. Bertrand, Mutations in the channel domain of a neuronal nicotinic receptor convert ion selectivity from cationic to anionic, Nature 359 (1992) 500–505.
[31] P.-J. Corringer, S. Bertrand, J.-L. Galzi, A. Devillers-Thiéry, J.-P. Changeux, D. Bertrand, Mutational analysis of the charge selectivity filter of the α7 nicotinic acetylcholine receptor, Neuron 22 (1999) 831–843.
[32] K. Imoto, C. Methfessel, B. Sakmann, M. Mishina, Y. Mori, T. Konno, K. Fukuda, M. Kurasaki, H. Bujo, Y. Fujita, S. Numa, Location of a delta-subunit region determining ion transport through the acetylcholine receptor channel, Nature 324 (1986) 670–674.
[33] S.P. Kelley, J.I. Dunlop, E.F. Kirkness, J.J. Lambert, J.A. Peters, A cytoplasmic region determines single-channel conductance in 5-HT_3 receptors, Nature 424 (2003) 321–324.
[34] S. Kumar, D. Bouzida, R.H. Swendsen, P.A. Kollman, J.M. Rosenberg, The weighted histogram analysis method for free energy calculations on biomolecules. 1. The method. J. Comput. Chem. 13 (1992) 1011–1021.
[35] B. Roux, The calculation of potential of mean force using computer simulations, Comput. Phys. Commun. 91 (1995) 275–282.
[36] A. Grossfield, http://membrane.urmc.rochester.edu.
[37] G.M. Torrie, J.P. Valleau, Monte Carlo free energy estimates using non-Boltzmann sampling: application to the sub-critical Lennard–Jones fluid, Chem. Phys. Lett. 28 (1974) 578–581.
[38] J.C. Phillips, R. Braun, W. Wang, J. Gumbart, E. Tajkhorshid, E. Villa, C. Chipot, R.D. Skeel, L. Kale, K. Schulten, Scalable molecular dynamics with NAMD, J. Comput. Chem. 26 (2005) 1781–1802.
[39] A.D. MacKerell Jr., D. Bashford, M. Bellott, R.L. Dunbrack Jr., J.D. Evanseck, M.J. Field, S. Fischer, J. Gao, H. Guo, S. Ha, D. Joseph-McCarthy, L. Kuchnir, K. Kuczera, F.T.K. Lau, C. Mattos, S. Michnick, T. Ngo, D.T. Nguyen, B. Prodhom, W.E.R. III, B. Roux, M. Schlenkrich, J.C. Smith, R. Stote, J. Straub, M. Watanabe, J. Wiórkiewicz-Kuczera, D. Yin, M. Karplus, All-atom empirical potential for molecular modelling and dynamics studies of proteins, J. Phys. Chem. B 102 (1998) 3586–3616.
[40] T. Darden, D. York, L. Pedersen, Particle mesh Ewald: an Nlog(N) method for Ewald sums in large systems, J. Chem. Phys. 98 (12) (1993) 10089–10092.
[41] U. Essmann, L. Perera, M.L. Berkowitz, T. Darden, H. Lee, L.G. Pedersen, A smooth particle mesh Ewald method, J. Chem. Phys. 103 (19) (1995) 8577–8593.
[42] B. Corry, T.W. Allen, S. Kuyucak, S.H. Chung, Mechanisms of permeation and selectivity in calcium channels, Biophys. J. 80 (2001) 195–214.
[43] S.C. Li, M. Hoyles, S. Kuyucak, S.H. Chung, Brownian dynamics study of ion transport in the vestibule of membrane channels, Biophys. J. 74 (1998) 37–47.
[44] S.H. Chung, T.W. Allen, S. Kuyucak, Conducting-state properties of the KcsA potassium channel from molecular and Brownian dynamics simulations, Biophys. J. 82 (2002) 628–645.
[45] M. Hoyles, S. Kuyucak, S.H. Chung, Solutions of Poisson's equation in channel-like geometries, Computer Phys. Commun. 115 (1998) 45–68.
[46] S. Chung, T. Allen, M. Hoyles, S. Kuyucak, Permeation of ions across the potassium channel: Brownian dynamics studies, Biophys. J. 77 (1999) 2517–2533.
[47] B. Corry, M. O 'Mara, S.-H. Chung, Conduction mechanisms of chloride ions in ClC-type channels, Biophys. J. 86 (2) (2004) 846–860.
[48] M. O 'Mara, B. Cromer, M. Parker, S.-H. Chung, Homology model of the GABAA receptor examined using Brownian dynamics, Biophys. J. 88 (5) (2005) 3286–3299.
[49] J.A. Ng, T. Vora, V. Krishnamurthy, S. -H. Chung, Estimating the dielectric constant of the channel protein and pore, Eur. Biophys. J. 37 (2008) 213–222.
[50] B. Corry, M. Hoyles, T.W. Allen, M. Walker, S. Kuyucak, S. -H. Chung, Reservoir boundaries in Brownian dynamics simulations of ion channels, Biophys. J. 82 (2002) 1975–1984.
[51] N.A. Baker, D. Sept, S. Joseph, M.J. Holst, J.A. McCammon, Electrostatics of nanosystems: application to microtubules and the ribosome, Proc. Natl. Acad. Sci. U. S. A. 98 (2001) 10037–10041.
[52] D. Petrey, Z. Xiang, C. Tang, L. Xie, M. Gimpelev, T. Mitros, C. Soto, S. Goldsmith-Fischman, A. Kernytsky, A. Schlessinger, Using multiple structure alignments, fast model building, and energetic analysis in fold recognition and homology modeling, Proteins 53 (2003) 430–435.
[53] O.S. Smart, J.G. Neduvelil, X. Wang, B.A. Wallace, M.S. Sansom, HOLE: a program for the analysis of the pore dimensions of ion channel structural models, J. Mol. Graph. 14 (1996) 354–360.
[54] W. Humphrey, A. Dalke, K. Schulten, VMD: visual molecular dynamics, J. Mol. Graph. 14 (1) (1996) 33–38.
[55] W. L. DeLano, The PyMOL Molecular Graphics System, DeLano Scientific, Palo Alto, CA, USA. URL http://www.pymol.org.
[56] B. Corry, Designing carbon nanotube membranes for efficient water desalination, J. Phys. Chem. B 112 (2008) 1427–1434.
[57] O.P. Hamill, B. Sakmann, Multiple conductance states of single acetylcholine receptor channels in embryonic muscle cells, Nature 294 (1981) 462–464.
[58] R.H. Meltzer, M.M. Lurtz, T.G. Wensel, S.E. Pedersen, Nicotinic acetyl-choline receptor channel electrostatics determined by diffusion-enhanced luminescence energy transfer, Biophys. J. 91 (2006) 1315–1324.
[59] S.B. Hansen, H.-L. Wang, P. Taylor, S.M. Sine, An ion selectivity filter in the EC-domain of cys-loop receptors reveals determinants for ion conductance, J. Biol. Chem. 283 (2008) 36066–36070.
[60] R.H. Meltzer, W. Vila-Carriles, J.O. Ebalunode, J.M. Briggs, S.E. Pedersen, Computed pore potentials of the nicotinic acetylcholine receptor, Biophys. J. 91 (2006) 1325–1335.
[61] G. Moy, B. Corry, S. Kuyucak, S.H. Chung, Tests of continuum theories as models of ion channels: I. Poisson–Boltzmann theory versus Brownian dynamics, Biophys. J. 78 (2000) 2349–2363.
[62] G. Brannigan, J. Henin, R. Law, R. Eckenhoff, M.L. Klein, Embedded cholesterol in the nicotinic acetylcholine receptor, Proc. Natl. Acad. Sci. U. S. A. 105 (2008) 14418–14423.
[63] D. Adams, T. Dwyer, B. Hille, The permeability of endplate channels to monovalent and divalent metal cations, J. Gen. Physiol. 75 (1980) 493–510.
[64] R.J.C. Hilf, R. Dutzler, X-ray structure of a prokaryotic pentameric ligand-gated ion channel, Nature 452 (2008) 375–380.
[65] R.J.C. Hilf, R. Dutzler, Structure of a potentially open state of a proton-activated pentameric ligand-gated ion channel, Nature 457 (2009) 115–119.
[66] N. Bocquet, H. Nury, M. Baaden, C.L. Poupon, J.-P. Changeux, M. Delarue, P.-J. Corringer, X-ray structure of a pentameric ligand-gated ion channel in an apparently open conformation, Nature 457 (2009) 111–114.